




## Nb<sub>2</sub>O<sub>5</sub> Pellets with Inactive Biomass for Adsorption of Mn<sup>2+</sup> Ions: Kinetic, Isothermal and Reuse Study

Tania Regina Giraldi<sup>a</sup>, Beatriz Caroline da Costa<sup>a</sup>, Marcos Martins Silva<sup>a</sup>, Allef Leite dos Santos<sup>b,c,\*</sup> ,  
Elaine Cristina Paris<sup>c</sup> , Alberthmeiry Teixeira de Figueiredo<sup>d</sup> , Renata Piacentini Rodriguez<sup>a</sup>

<sup>a</sup>Universidade Federal de Alfenas, Rodovia José Aurélio Vilela, 11.999, 37715-400, Poços de Caldas, MG, Brasil.

<sup>b</sup>Universidade de São Paulo (USP), Instituto de Química de São Carlos, Avenida Trabalhador São Carlense, 400, 13566-590, São Carlos, SP, Brasil.

<sup>c</sup>Embrapa Instrumentação Agropecuária, Laboratório de Nanotecnologia para o Agronegócio (LNNA), Rua XV de Novembro, 1452, 13560-970, São Carlos, SP, Brasil.

<sup>d</sup>Universidade Federal de Catalão, Av. Dr. Lamartine Pinto de Avelar, 1120, Setor Universitário, 75704-020, Catalão, GO, Brasil.

Received: December 16, 2022; Revised: March 06, 2023; Accepted: March 30, 2023

This paper aims to explore the production of porous Nb<sub>2</sub>O<sub>5</sub> pellets by pressing and adding anaerobic biomass (sludge) in order to evaluate the microstructure porosity. The thermal treatment temperature of the pellets varied between 300 °C and 900 °C. Their structural, morphological, and physical properties were measured, and the adsorption potential of Mn<sup>2+</sup> and their reuse were evaluated. All samples had a monoclinic phase. Density average values of samples pressed using sludge ranged between 2.45 and 2.52 g.cm<sup>-3</sup>, while the one obtained without sludge pressing achieved higher values of around 2.72 g.cm<sup>-3</sup>. All samples presented high porosity values after the heat treatment (above 40%), which confirms the efficiency of sludge as a means to enhance porosity. These pellets were used for Mn<sup>2+</sup> ions adsorption in aqueous medium. The Langmuir isotherm model was the one that achieved the best goodness-of-fit. In kinetic studies, the adsorption reaction was in accordance with second-order kinetics. Adsorbents in the form of pellets are environmentally friendly on account of their significant reuse and recycling potential. However, the particulate matter might become an environmental liability and incur high treatment costs. The samples proved to be reusable, promoting the adsorption of 67% of the Mn<sup>2+</sup> after the fifth reuse cycle.

**Keywords:** Nb<sub>2</sub>O<sub>5</sub>, pellets, adsorption, reuse, Mn<sup>2+</sup>.

### 1. Introduction

Proper access to water is essential to foster socioeconomic development, as there might be direct effects on the health conditions and well-being of the population, which is increasingly critical in multiple regions of the planet. Given the need for its conservation and sustainable development, measures must be sought and developed to minimize waste generation, avoid inappropriate waste disposal into these water bodies, and promote decontamination of polluted aquatic environments. Among pollutants found in aqueous media, heavy metals are worth mentioning, some of which are Zn<sup>2+</sup>, Co<sup>2+</sup>, Cu<sup>2+</sup>, and Mn<sup>2+</sup>. They can be found in nature (soil, air, and water) and food and are considered essential microelements for regulating the metabolism of living organisms<sup>1</sup>. However, their excess or lack can affect such organisms and even lead to death in more severe cases due to the formation of complexes with functional groups of enzymes in living beings<sup>2</sup>.

There are several methods for removing heavy metal ions from aqueous media, such as adsorption, which is a promising and highly efficient process in this regard.

Metallic oxides can be suitable adsorbents as they can be easily obtained at a low cost<sup>3</sup>. These materials are practically insoluble in water, but they still have robust structures, given that they suffer slight expansion or compression when immersed in an aqueous solution, i.e., essential characteristics for achieving good performance as adsorbents<sup>4</sup>.

The literature reports different types of adsorbents. Specifically, for Mn<sup>2+</sup> adsorption, some studies evaluated the removal directly from wastewater. Ajala et al.<sup>5</sup> evaluated the adsorptive behavior of rutile-phased titania nanoparticles supported on acid-modified kaolinite clay to remove selected heavy metal ions from mining wastewater. In the results, the authors verified removing 57% of Mn<sup>2+</sup> from the environment under these conditions. Fikri et al.<sup>6</sup> studied the thickness variations effect of zeolite and activated carbon media adsorbent in reducing phenol and manganese levels of non-destructive testing wastewater. The thickness of adsorbates varied between 40 and 80 cm, and a maximum Mn<sup>2+</sup> reduction of 80% was obtained. Mubarak<sup>7</sup> evaluated the removal of excess heavy metal ions and hardness from groundwater in a highly localized contaminated area using TiO<sub>2</sub>@Zeolite nanocomposite.

\*email: allef.leitte@gmail.com

The maximum recovery efficiencies of  $Mn^{2+}$  ions were 100% using the adsorbent studied. Vasiraja<sup>8</sup> evaluated the adsorption efficiency of activated carbon derived from *Prosopis juliflora* stem to remove heavy metal-containing textile industry effluent. In this study, the  $Mn^{2+}$  removal efficiency was 71.42%.

Among several metal oxides,  $Nb_2O_5$  has been attracting increased attention in the field of catalysis<sup>9-13</sup> nowadays, often with the purpose of being used in environmental remediation, such as photocatalysis<sup>14</sup>. However, there are few studies in the literature on the use of  $Nb_2O_5$  as adsorbent material for metallic ions. Costa et al.<sup>15</sup> analyzed the viability of coupling  $Nb_2O_5$  with  $Al_2O_3$  in the form of a solid substrate on a silica matrix prepared by the sol-gel process to use as an adsorbent of  $Cd^{2+}$  ions. The material showed great stability, and the obtained results by modifying porous silica using oxide metals are pretty promising for developing new materials able to adsorb metal ions. Diniz et al.<sup>16</sup> synthesized  $Nb_2O_5$  coupled with ZnO dispersed in a silica matrix by the sol-gel method and used it as an adsorbent of cobalt ions ( $Co^{2+}$ ) found in water and food samples. Yang et al.<sup>17</sup> analyzed the ratio of the binary compound  $Nb_2O_5/TiO_2$  synthesized by the sol-gel method and investigated the adsorption/catalytic combustion of 1,2-dichloroethane (DCE). The material showed high porosity and a large diameter ranging between 2-10 nm.

In the aforementioned studies, suspended adsorbent particles were placed/immersed in a liquid medium, thus achieving a large surface area and good efficiency in mass transfer processes. Although some publications reveal the use of these materials as nanometric powders, a lack of practicality of this particular method is noteworthy given that if the adsorbent powder is not well fixed on a given support, the material might be dragged, and the process effectiveness is thus compromised, as new steps are also entailed in the treatment<sup>18</sup>. Moreover, it is difficult to separate adsorbate particles from the reaction medium at the end of the process. Eliminating the step of adsorbate separation decreases the time taken to complete the process, in addition to facilitating industrial-scale applications. Furthermore, the production and use of pressed samples also offer the advantage of being reused in various reaction cycles. A conformation of powders eventually leads to a reduced surface area, which is disadvantageous given that these materials are regarded as pellets. Therefore, alternatives are sought to produce porous materials, such as the incorporation of organic compounds inside ceramic materials<sup>19-21</sup>. This method consists basically in dispersing organic compounds within an oxide through the preparation of a homogeneous biphasic mixture in such a way that, during the process of heat treatment, such compounds are eliminated, thus leaving a group of pores. In this work, anaerobic granular sludge was used as a material in order to enhance porosity. It corresponds to granular biomass from a UASB reactor used to treat effluents from poultry slaughterhouses (Avicultura Dacar, Tietê - SP). For such a purpose,  $Nb_2O_5$  sludge pellets were obtained and subjected to different heat treatment temperatures. These pellets were used to remove  $Mn^{2+}$  ions from aqueous solutions, and the influence of heat treatment temperature on physical, structural, and adsorptive properties of  $Nb_2O_5$  pellets was assessed, in addition to an investigation into the kinetics and adsorption isotherm of  $Mn^{2+}$ . Their reuse capability was also evaluated through five adsorption cycles.

## 2. Experimental

### 2.1. Biomass characterization

Initially, the biomass was subjected to drying at 150 °C to eliminate moisture. Then, it was subject to thermogravimetric analysis (TGA) to identify mass variations and thermal stability. Measurements were performed on Jupiter® model STA 449 F3, using a temperature range of 20–800 °C and a standard heating rate of 10 °C.min<sup>-1</sup>. The sample was placed in an alumina crucible, and synthetic air was used as the purge gas with a standard flow of 100 mL.min<sup>-1</sup>. The material was characterized by FTIR before and after the thermogravimetric analysis to verify its stability and change in its composition after the heat treatment. FTIR analysis was carried out using an Agilent Cary 630 FTIR Spectrometer in attenuated total reflectance (ATR) mode whose wavelength range between 4000 and 500 cm<sup>-1</sup> and resolution of 4 cm<sup>-1</sup>.

### 2.2. Obtaining and characterizing pellets

$Nb_2O_5$  pellets were prepared by pressing a mixture of 95% of  $Nb_2O_5$  powder, and 5% of granular biomass from a UASB reactor used to treat effluents from poultry slaughterhouses (Avicultura Dacar, Tietê - SP).  $Nb_2O_5$  powder was kindly donated by CBMM, identified as HY-340R herein. 2.5 g of this mixture was added into a stainless steel mold with an opening diameter of 2 cm. The mold was subjected to uniaxial pressing, whose applied strength was 12.88 MPa (N.mm<sup>-2</sup>), equivalent to 2 tons. After obtaining the pellets, heat treatments were carried out at different temperatures: 300 °C, 400 °C, 500 °C, 600 °C and 900 °C, in an EDG 3000 muffle furnace for 2 hours at a heating and cooling rate of 1 °C.min<sup>-1</sup>. Pure  $Nb_2O_5$  (without sludge) was also obtained to carry out comparative studies from results for pellets treated at 900 °C. These samples were coded as *T* or *T\**, where *T* is temperature and the asterisk indicates the presence of biomass.

XRD analyses were performed on a Shimadzu XRD-6100 diffractometer at 30 kV and 30 mA using Cu-K $\alpha$  radiation and a graphite monochromator in a range from 5 to 85°. FTIR analysis was carried out using a Cary 630 FTIR Spectrometer (Agilent) equipment in attenuated total reflectance (ATR) mode, whose wavelength range between 4000 and 500 cm<sup>-1</sup> and resolution of 4 cm<sup>-1</sup>. The microstructure of samples was evaluated using a scanning electron microscope, model JEOL JSM 6701F. Zeta potential analyses were performed in a  $Nb_2O_5$  pellet portion. The pellet surface portion was scraped, and 2 mg of the collected powder was analyzed using a Malvern Instruments Zetasizer Nano. Experiment preparation consisted of dispersing 2 mg of sample in 10 mL of Milli-Q in KCl solution, prepared from high-purity reagents, using a Branson Digital Sonifier. The solution pH was adjusted to 6.0.

Apparent porosity (AP) and apparent density (AD) were determined using a method based on Archimedes' principle, according to ASTM C20-00 (Reapproved in 2010), calculated from experimental data using Eqs. (1) and (2). The experimental procedure was initially aimed to measure the dry weight ( $W_d$ ) of pellets after the heat treatment.

Then, the samples were immersed in beakers containing water at room temperature for 24 h. Afterward, their immersed weight ( $W_i$ ) was determined. Finally, the samples were removed from the water and weighed again while they were still wet to calculate their wet weight ( $W_w$ ). All weight measurements were performed on a semi-analytical scale (Shimadzu AY220).

$$AP(\%) = \frac{W_w - W_d}{W_w - W_i} \times 100 \quad (1)$$

$$AD(g\text{ cm}^{-1}) = \frac{W_d}{W_w - W_i} \times d_{\text{water}} \quad (2)$$

### 2.3. Mn<sup>2+</sup> adsorption studies

Mn<sup>2+</sup> adsorption studies were carried out at room temperature, using aqueous solutions of Mn<sup>2+</sup> ions (adsorbate) prepared by Manganese(II) acetate tetrahydrate ((CH<sub>3</sub>COO)<sub>2</sub>Mn·4H<sub>2</sub>O, Vetec™). Experiments were conducted in triplicate, starting from an immersion of the pellet in 50 mL of a 50 mg.L<sup>-1</sup> Mn<sup>2+</sup> solution in 250 mL beakers sealed with a plastic wrap and kept under stirring at 150 rpm and 30° C in a thermostatic shaker incubator (SL-221, Solab). Mn<sup>2+</sup> concentration in the supernatant was determined using a High-Resolution Atomic Absorption Spectrophotometer (ContraAA®300 Analytik Jena) operating with synthetic air/acetylene flame. Experiments were initially performed in order to determine the pellet that had achieved the best adsorptive capacity by fixing contact time at 1 hour using solutions containing 50 mg.L<sup>-1</sup> of adsorbate, whose pHs were set at 6.0 (the natural pH of the manganese acetate solution). The idea was to maintain the study solution's natural pH to evaluate the efficiency of the pellets with the least possible changes in the system. Notably, after the adsorption process, there was no change in pH. Results were checked for statistical significance using a student t-test at the 0.05 confidence level. This analysis was applied to evaluate the influence of heat thermal temperature of the pellets on adsorption percentage. Statistical analyses were carried out using Microsoft Excel.

The sample obtained at 300 °C was selected to study adsorption kinetics and the isotherm. Then, a kinetics

study was carried out using aqueous adsorbate solutions of 50 mg.L<sup>-1</sup> with contact times set at 1, 3, 5, 10, 20, 30, 45 and 60 minutes. Adsorption isotherm study was carried out at adsorbate concentrations of 10, 15, 20, 50, 75, 100, and 150 mg.L<sup>-1</sup> in aqueous solutions. Lastly, five cycles of adsorption and desorption assays were performed. Experiments were conducted, starting from a pellet immersion in 50 mL of a 50 mg.L<sup>-1</sup> Mn<sup>2+</sup> solution in 250 mL beakers sealed with a plastic wrap and kept under stirring at 150 rpm 30 °C and 1 h in a thermostatic shaker incubator (SL-221, Solab). The pellets were immersed in 50 mL of deionized water for desorption experiments and maintained under the same experimental conditions as the adsorption tests. Mn<sup>2+</sup> concentration in the supernatant was determined using a High-Resolution Atomic Absorption Spectrophotometer (ContraAA®300 Analytik Jena) operating with synthetic air/acetylene flame.

## 3. Results and Discussion

### 3.1. Biomass characterization

Initially, the raw biomass was subjected to drying at 150 °C to remove moisture to enable its use in the development of pellets. Subsequently, it was submitted to a differential thermal analysis (TG) at 800 °C (Figure 1a). The curve of the sludge showed a rapid decline, indicating mass loss as a function of increasing temperature. This loss was significant, with approximately 82% mass loss up to 580 °C, which was associated with sludge decomposition at high temperatures. The derived thermogravimetric curve (DTG) is associated with the derivative of the TG curve, where the steps of the TG curve are replaced by peaks that delimit areas proportional to the mass changes in the sample. Three peaks were observed, where the loss of mass occurred more intensely at temperatures of 220, 454, and 612 °C, while up to 150 °C, there was a loss of water, and up to 250 °C, the loss of mass was related to the decomposition of organic matter.

Figure 1b shows FTIR spectra of the slurry drying at 150 °C and heat treated at 800 °C. It can be observed that there is a characteristic band of O-H groups at 3250 cm<sup>-1</sup> originating from wastewater for the sample treated at 150 °C.

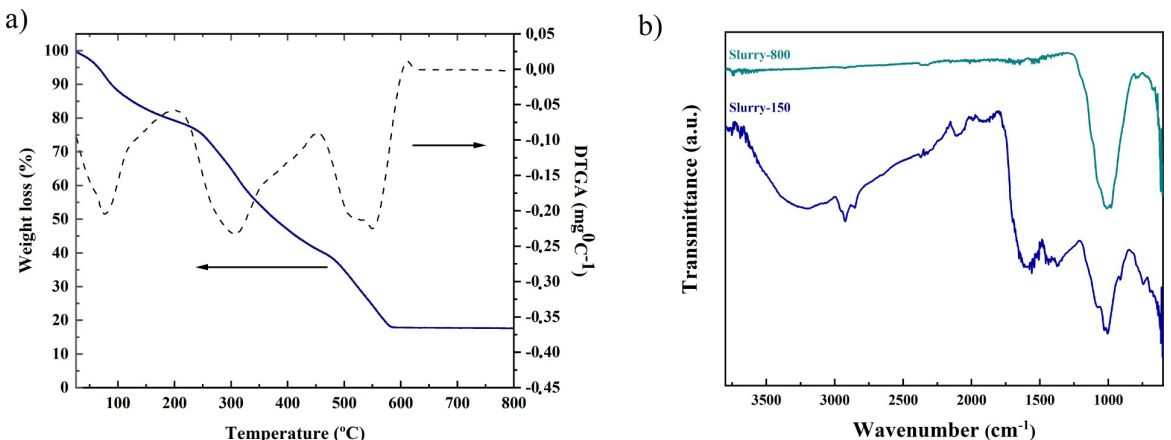


Figure 1. (a) Sludge thermogram and (b) FTIR spectra of the sludge drying at 150°C and heat treated at 800 °C.

At  $2960\text{ cm}^{-1}$  and  $2925\text{ cm}^{-1}$ , there are two distinct bands of methyl and methylene groups. It is still observed aliphatic C-H stretching groups at  $2900\text{ cm}^{-1}$ . The band at  $1634\text{ cm}^{-1}$  is typical of primary amides, and there is a band corresponding to secondary amide groups at  $1541\text{ cm}^{-1}$ . At  $1027\text{ cm}^{-1}$ , there are bands associated with hydroxyl groups. The band at around  $1000$  and  $1100\text{ cm}^{-1}$  can be attributed to the C-O bond stretching frequency. Comparing the FTIR results of sludge heat-treated at  $800\text{ }^{\circ}\text{C}$  with the one treated at  $150\text{ }^{\circ}\text{C}$ , the influence of temperature on functional groups present in sludge can be evidenced since there is a characteristic band at  $1100\text{ cm}^{-1}$  only after temperature increase.

### 3.2. Pellets characterization

The X-ray diffractograms shown in Figure 2a were obtained for the pellets whose diffraction pattern resembles the monoclinic phase of  $\text{Nb}_2\text{O}_5$ , according to the *Joint Committee on Powder Diffraction Standards* (JCPDS, n° 72-1121). Samples of pellets were heat-treated at  $300$ ,  $400$ ,  $500$ ,  $600$ , and  $900\text{ }^{\circ}\text{C}$ . At  $900\text{ }^{\circ}\text{C}$  without sludge, it shows characteristic peaks only in the monoclinic phase.

These results indicate that the heat treatment has not altered the crystalline structure of  $\text{Nb}_2\text{O}_5$ . No characteristic peaks of charcoal were identified, given such a small amount of this compound in the final composition. It is worth mentioning that  $5\%$  (m/m) of mass was initially added, corresponding to  $0.125\text{ g}$  of biomass. According to thermogravimetric results,  $18\%$  of its mass remained, i.e.,  $0.023\text{ g}$ , which corresponds to  $\sim 1.0\%$  of the total mass of the pellet, but such an amount is below the detection limit of the device. Therefore, it was not possible to identify charcoal residues by XRD. The same is found while analyzing the FTIR spectra presented in Figure 2b. It is observed that, although there is temperature variation, there were no significant changes on the surface of the pellets. At wavelengths ranging from  $500$  to  $1000\text{ cm}^{-1}$ , there are characteristic bands of niobium-oxygen (Nb-O) bonds. It can be observed that wavelengths remain constant even as the heat treatment temperature increases.

On the other hand, when analyzing the images obtained by SEM (Figure 3), it is observed that some samples are composed of fibers, thus evidencing the presence of inorganic residues from the sludge.

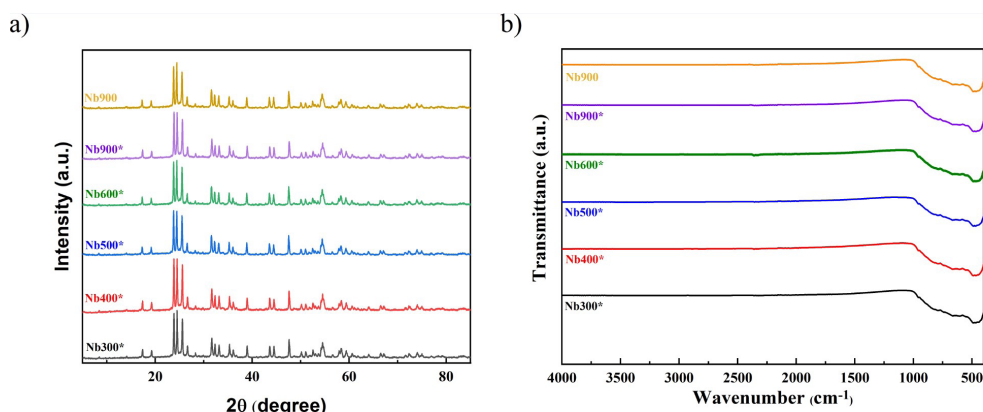


**Figure 2.** (a) X-ray diffraction patterns and (b) FTIR spectra of pellets obtained in different temperature. Samples obtained with sludge are represented with a \*.

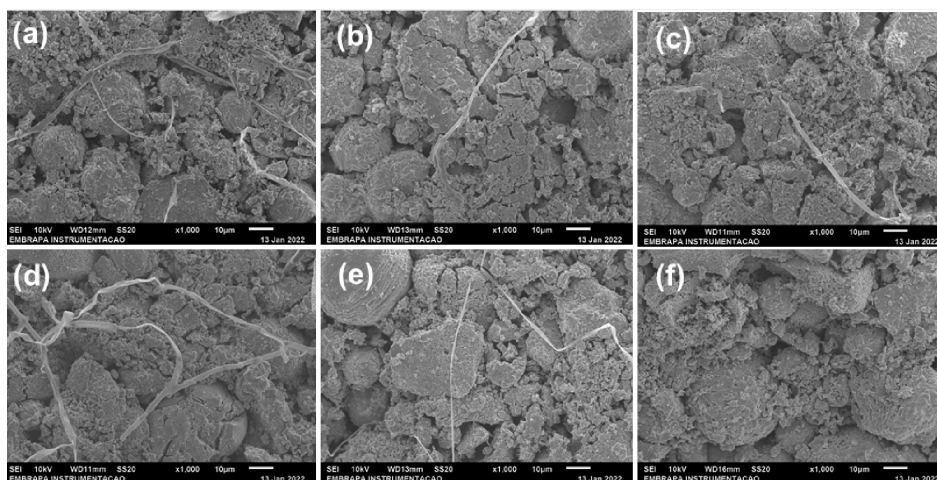


**Figure 3.** SEM images of  $\text{Nb}_2\text{O}_5$  pellets at  $1000\times$  magnification (a)  $300^{\circ}\text{C}$ , (b)  $400^{\circ}\text{C}$ , (c)  $500^{\circ}\text{C}$ , (d)  $600^{\circ}\text{C}$ , (e)  $900^{\circ}\text{C}$  and (f)  $900^{\circ}\text{C}$  without sludge.

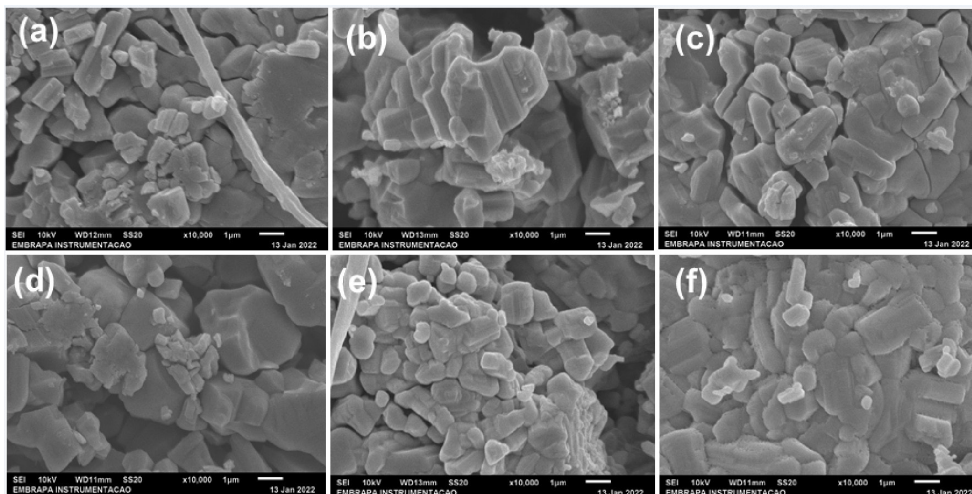


Figure 4 shows SEM images of their surface at greater magnification so as to analyze the morphology of grains. It is observed that samples have an undefined morphology varying greatly in size. As for the sample pressed with sludge, it is possible to observe some pores between grains, which can be explained by the decomposition of sludge present in the sample. It is also observed that there is no regularity in the morphology of samples treated at temperatures ranging from 300 to 600 °C.

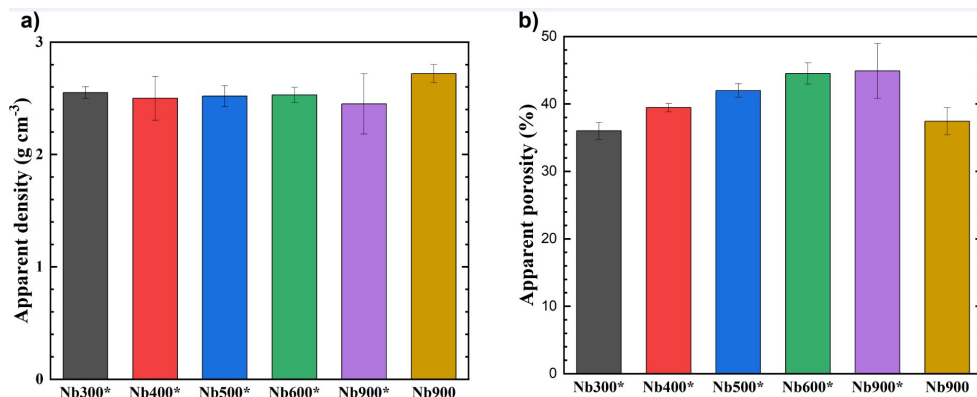
Grain growth is related to its packing since the grain boundary movement rate is proportional to the rate of movement of atoms across boundaries<sup>21</sup>. The samples were obtained by uniaxial pressing, which explains the densification and agglomeration of grains, as can be seen in Figure 4f, which reveals that the sample treated at 900 °C contains only Nb<sub>2</sub>O<sub>5</sub>. In other samples, such a profile was not observed due to the presence of sludge. Although only residues of the samples were detected in their final composition, the presence of sludge during the initial stages of the heat treatment prevented contact between Nb<sub>2</sub>O<sub>5</sub> grains, which generated pores in samples.

Figure 5a, 5b shows the apparent densities and porosities found for the pellets. In Figure 5a, it is possible to observe that the apparent densities of samples pressed with sludge at values ranging between 2.45 and 2.52 g.cm<sup>-3</sup> have reached lower values than the theoretical density of 4.95 g.cm<sup>-3</sup> for Nb<sub>2</sub>O<sub>5</sub><sup>22</sup>, while the sample obtained without sludge reached higher values of 2.72 g.cm<sup>-3</sup> on average.

Bulk density makes open pores susceptible to water penetration. Thus, its increase is related to a decrease in the amount of open pores in the structure due to better packing<sup>23</sup>. The sample treated at 900 °C without sludge showed greater bulk density due to the absence of organic matter, which allowed further contact between the grains. Regarding the behavior of samples towards apparent porosity, as shown in Figure 5b, porosity values obtained for samples pressed with sludge increased gradually as heat treatment temperatures rose from 300 °C to 600 °C, i.e., from 36 to 44%. After this temperature range, porosity remained constant at 44%. This reveals that the heat treatment allowed gradual sludge decomposition, thus generating new pores in pellets.



**Figure 4.** SEM images of Nb<sub>2</sub>O<sub>5</sub> pellets at 10000x magnification (a) 300°C, (b) 400°C, (c) 500°C, (d) 600°C, (e) 900°C and (f) 900°C without sludge.



**Figure 5.** (a) Apparent density and (b) apparent porosity of pellets obtained in different temperature. Samples obtained with sludge are represented with a \*.

After 600 °C, the decomposition of the organic matter ended, thus sample porosity treated at 600 °C and 900 °C remained practically constant. As for the sample obtained at 900 °C without sludge, the porosity value was 37.4%, i.e., a lower porosity value than that of the sample treated at 900 °C with sludge (44.9%). The fact of not using sludge allowed grains to have greater contact with each other from the initial temperatures of the heat treatment, which in turn promoted the densification of pellets and, consequently, a reduction in their porosity. As for the sample treated at 900 °C with sludge, there is greater porosity due to the pores left in the in-between of grains by sludge while it decomposes, thus making it difficult to densify the pellet.

### 3.3. Adsorption tests

Initially, adsorption tests were performed on samples obtained at different temperatures, whose results are shown in Figure 6.

The adsorption percentage ranged between 63.3 and 67% among samples. The sample obtained at a lower temperature (300 °C) showed 65% adsorption, but the one obtained at a higher temperature (900 °C) showed 67% adsorption. By comparing the sample with sludge to the one without sludge, obtained at the same temperature (900 °C), it is observed that the one with sludge showed higher adsorption percentages than the one without sludge. Such a difference can be explained by the fact that the sample obtained with sludge has a greater amount of pores than the one without sludge. This is due to the presence of sludge during the initial heat treatment stages, which in turn prevented contact between Nb<sub>2</sub>O<sub>5</sub> grains and generated pores in the samples.

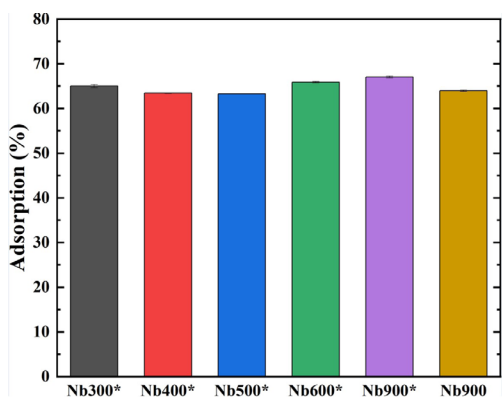


Figure 6. Adsorption percentage of Mn<sup>2+</sup> on the pellets obtained at different temperature. Samples obtained with sludge are represented with a \*.

This leads to samples having greater porosity, as evidenced in the apparent porosity analysis (Figure 5b) and SEM (Figure 4).

The analysis of the effect of temperature on the adsorption percentage was confirmed with the application of the t-test (Table 1), which indicated a statistically significant impact of temperature on the adsorption capacity (p-value < 0.05), except for the comparison between the temperature of 300 °C with 600 °C and 400 °C with 500 °C.

Usually, the mechanism of the heavy metal ions' adsorption onto the oxide adsorbents is greatly influenced by the surface chemistry of the adsorbent, the ionic charge on the metal ions, and the adsorbate interactions<sup>24</sup>. To better understand the adsorption mechanism, zeta potential analysis of Nb<sub>2</sub>O<sub>5</sub> was performed at pH 6.0. At this pH, the zeta potential value was -45 mV, which indicates that the surface charge of the Nb<sub>2</sub>O<sub>5</sub> becomes highly negative. These results suggest that at the pH used in the present study, the surface of Nb<sub>2</sub>O<sub>5</sub> pellets contains basic groups, possibly oxygen ions (O<sup>-</sup>), promoting electrostatic attraction and favoring adsorption, which facilitates the approximation of Mn<sup>2+</sup> cations. In addition, it is believed that the presence of pores favors the penetration of Mn<sup>2+</sup> into the sample, making the adsorption process more efficient.

In view of preliminary results, the sample obtained at 300 °C was selected for studying adsorption kinetics and the adsorption isotherm. This sample was selected as there was no significant difference regarding the percentage of adsorption of other samples. However, lower heat treatment temperatures provide greater feasibility for using this material on a large scale. Thus, the Nb<sub>2</sub>O<sub>5</sub> pellet obtained at 300 °C allowed for studying the influence of contact time between pellets in a 50 mg.L<sup>-1</sup> Mn<sup>2+</sup> solution on the adsorptive process. The adsorption results as a function of contact time can be seen in Figure 7

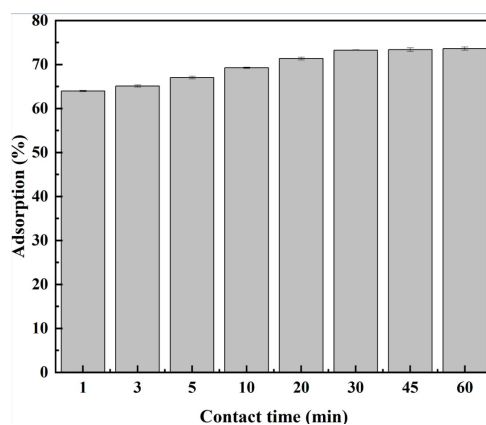


Figure 7. Adsorption percentage as a function of contact time using.

Table 1. p-values for the adsorption percentage.

Apparent porosity (p-value)	Nb300*	Nb400*	Nb500*	Nb600*	Nb900*	Nb900
Nb300*		0.018	0.014	0.062	0.014	0.047
Nb400*			0.081	0.0018	0.0015	0.04
Nb500*				0.014	0.0013	0.021
Nb600*					0.018	0.005
Nb900*						0.003
Nb900						

At first, it is observed that adsorption occurs more quickly during the first minutes of contact, i.e., 64% of ions are adsorbed on the pellet within just 1 minute. As soon as the initial minutes, the adsorption speed gradually decreased, which might be attributed to the availability of active sites available at the beginning of the process, which are occupied as the equilibrium of the ion exchange is reached over time, thus reflecting a lower adsorption rate over time. This behavior is reflected in the shape of the experimental adsorption curve ( $q_t \times \text{time}$ ), as seen in Figure 8, showing a rapid increase in initial times indicated by the high slope of the curve and then a low slope until reaching equilibrium. It is also observed that adsorption/desorption equilibrium was reached within 45 minutes. Thus, afterward, the Mn<sup>2+</sup> concentration in the solution remains constant. These experimental data were fitted to pseudo-first and pseudo-second-order kinetic models in order to verify the adsorption kinetic model. Figures 8 show the model curves fitted to the experimental data.

Based on the adjustment and non-linear regression models, it was possible to obtain the parameters of pseudo-first and pseudo-second order equations<sup>25</sup>, namely adsorption capacity at equilibrium ( $q_e$ ) and adsorption rate constants ( $k$ ). In addition, the R<sup>2</sup> coefficient of determination was calculated for each of the models. These data can be found in Table 2.

By analyzing adjustments to experimental data and the coefficients of correlation of each model, it can be observed that the pseudo-second-order model was a better fit to the experimental data obtained while analyzing based on R<sup>2</sup> since they are closer to a unit value of 1, i.e., characteristic of a model achieving the perfect fit. In addition, the value of  $q_e$  calculated by the methods is quite consistent with experimental data. The adsorption capacity of the sample found by the method reached a value of 35.9 mg/g in comparison with 37.0 mg/g, which was obtained experimentally. Thus, the pseudo-second-order kinetic model proves to achieve goodness-of-fit based on R<sup>2</sup> and the adsorption capacity at equilibrium, as it is consistent with results obtained experimentally.

As regards the adsorption isotherm study, there were varying Mn<sup>2+</sup> concentrations, i.e., 10, 30, 50, 70, 90, and 110 mg.L<sup>-1</sup>. Adsorption data were fitted using Langmuir and Freundlich isotherm models<sup>25</sup>. From the data shown in Table 3, a graph was plotted to depict initial concentrations of Mn<sup>2+</sup> as a function of adsorption capacity at equilibrium, i.e.,  $q_e$  in mg/g, and the final solution concentration after reaching equilibrium, i.e.,  $C_e$  in mg/L. The graph in Figure 9 shows the adjustments for Langmuir and Freundlich isotherm models.

The coefficients of correlation of isotherms reveal that the Langmuir model better describes adsorption data since the R<sup>2</sup> value was 0.99. Through the value of  $Q_{\text{max}}$ , it was observed that the highest adsorption capacity of the pellet is 2.04 mgg<sup>-1</sup>. These values are close to the experimentally found value of 1.66 mgg<sup>-1</sup>, which indicates that the results found fulfill expectations. The constants of isotherms characterize the adsorption parameters of the adsorbent material.

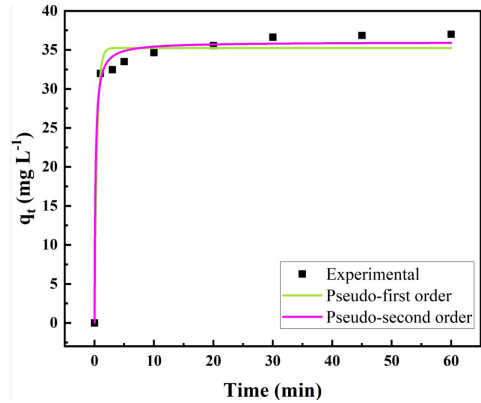


**Figure 8.** Experimental adsorption kinetics of Mn<sup>2+</sup> and the adjustment of first- and second-order kinetic models to data on the pellet obtained at 300°C.

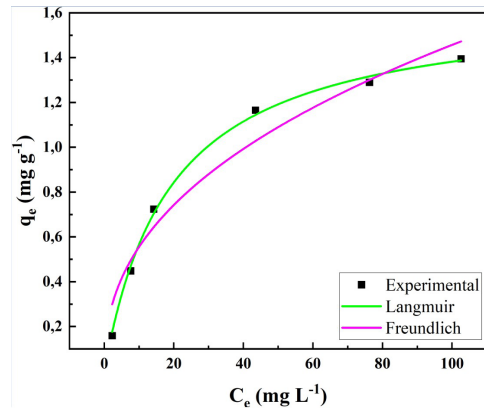


**Figure 9.** Experimental data and adjustments of Langmuir, Freundlich Isotherm models for Mn<sup>2+</sup> ions adsorption on the pellet obtained at 300°C.

**Table 2.** Values obtained in pseudo-first and pseudo-second order models.

Pseudo-first order			Pseudo-second order		
$q_e$ (mg.g <sup>-1</sup> )	$k$ (g.min.mg <sup>-1</sup> )	R <sup>2</sup>	$q_e$ (mg.g <sup>-1</sup> )	$k$ (g.min.mg <sup>-1</sup> )	R <sup>2</sup>
35.2	2.3542	0.9831	35.9	0.1699	0.9917

**Table 3.** Data obtained for the adjustments of Langmuir and Freundlich isotherms.

Langmuir			Freundlich		
$Q_{\text{max}}$ (mg.g <sup>-1</sup> )	$K_L$ (L.mg <sup>-1</sup> )	$R_L$	$K_f$	$N$	R <sup>2</sup>
1.64	0.05	0.99	0.21	2.38	0.96

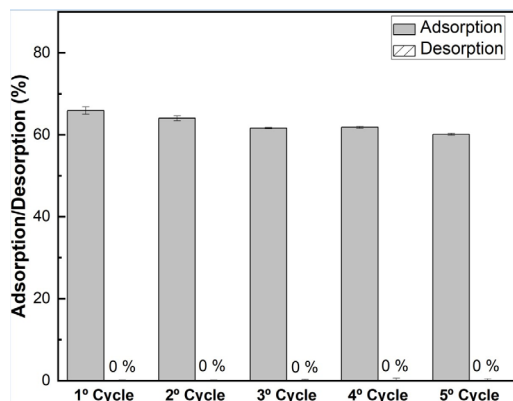


**Figure 10.**  $Mn^{2+}$  adsorption and desorption cycles on the pellet obtained at  $300^{\circ}C$ .

For both samples, the value of  $R_L$  indicates that adsorption is a favorable process ( $0 < R_L < 1$ ) in the studied concentration range for the prepared material since the  $R_L$  value found was 0.92. As for the Freundlich adjustment, there are  $n$  values of 2.38, which reveal that adsorption is favorable since values of  $n$  range between 1 and 10.

Finally, the pellets were applied in 5 adsorption and desorption cycles of  $50 \text{ mg}\cdot\text{L}^{-1}$   $Mn^{2+}$  solutions to evaluate the reuse of pellets. These results are shown in Figure 10.

By analyzing the data shown in Figure 10, it is observed that 65% of adsorption was in the first cycle. This percentage is slightly reduced throughout cycles, reaching 60% in the fifth. Thus, the pellets prove to be reusable since the adsorption value is reduced by an average of 5% from the first to the last cycle for the sample, which can be explained by the fact that the material itself is capable of retaining ions. Furthermore, there was no  $Mn^{2+}$  desorption in any cycle. Concerning the reuse evaluation, the pellets maintained adsorptive activity even without desorption, with a slight decrease in adsorption percentage over the cycles. This behavior can be attributed to the high porosity, favoring the  $Mn^{2+}$  ions' diffusion to more internal pellet regions. In addition, it is important to evidence that the presence of pores improves the penetration of ions in the interior of the samples, which makes the adsorption process more efficient. Thus, it is evident that the pellet presents stability in retaining  $Mn^{2+}$  ions, and its potential for application and development of adsorbents to remove metallic ions is thus evidenced.

## 4. Conclusion

$Nb_2O_5$  with anaerobic biomass (sludge) pellets obtained by the pressing technique have been successfully used in the adsorption of  $Mn^{2+}$  ions. Apparent density values for samples pressed with sludge reached average values ranging between  $2.45$  and  $2.52 \text{ g}\cdot\text{cm}^{-3}$ , while the sample obtained without sludge achieved higher values of  $2.72 \text{ g}\cdot\text{cm}^{-3}$ . All samples presented high porosity values after the heat treatment, which confirms the efficiency of sludge in enhancing porosity as porous bodies maintained their integrity. A factorial design of experiments was adopted and statistical analysis was performed in the form of ANOVA and student "t" test,

which gave good interpretation in terms of interaction of experimental parameters. The adsorption mechanism was in accordance with second-order kinetics and Langmuir adsorption isotherm. Pellets were easily removed from the medium and showed good reusability for up to five adsorption cycles. During reuse cycles, pellets were chemically and thermally stable and had sufficient mechanical strength for  $Mn^{2+}$  removal. Adsorbents in pellet form are environmentally friendly on account of their great reuse and recycling potential. In contrast, the particulate matter might become an environmental liability and incur high treatment costs.

## 5. Acknowledgments

The authors thank the Brazilian research funding agencies CAPES (Finance code 001), CNPq and FAPEMIG (37590960/2021). They are also grateful to CBMM (Brazilian metallurgy and mining company) for donating the HY-340R.

## 6. References

- Sall ML, Diaw AKD, Gningue-Sall D, Efremova Aaron S, Aaron JJ. Toxic heavy metals: impact on the environment and human health, and treatment with conducting organic polymers, a review. *Environ Sci Pollut Res Int.* 2020;27(24):29927-42. <http://dx.doi.org/10.1007/s11356-020-09354-3>.
- Rahman Z. An overview on heavy metal resistant microorganisms for simultaneous treatment of multiple chemical pollutants at co-contaminated sites, and their multipurpose application. *J Hazard Mater.* 2020;396:122682. <http://dx.doi.org/10.1016/j.jhazmat.2020.122682>.
- Ali Redha A. Removal of heavy metals from aqueous media by biosorption. *Arab J Basic Appl Sci.* 2020;27(1):183-93. <http://dx.doi.org/10.1080/25765299.2020.1756177>.
- Wang L, Shi C, Pan L, Zhang X, Zou JJ. Rational design, synthesis, adsorption principles and applications of metal oxide adsorbents: a review. *Nanoscale.* 2020;12(8):4790-815. <http://dx.doi.org/10.1039/C9NR09274A>.
- Ajala MA, Abdulkareem AS, Tijani JO, Kovo AS. Adsorptive behaviour of rutile phased titania nanoparticles supported on acid-modified kaolinite clay for the removal of selected heavy metal ions from mining wastewater. *Appl Water Sci.* 2022;12(2):1-24. <http://dx.doi.org/10.1007/s13201-021-01561-8>.
- Fikri E, Mutiara Farid R, Septiati Y, Djuhriah N, Hanurawaty N, Khair A. Effect of zeolite and activated carbon thickness variation as adsorbent media in reducing phenol and manganese levels in wastewater of non-destructive testing Unit. *J Ecol Eng.* 2022;23(8):40-8. <http://dx.doi.org/10.12911/22998993/150653>.
- Mubarak MF, Mohamed AMG, Keshawy M, elMoghny TA, Shehata N. Adsorption of heavy metals and hardness ions from groundwater onto modified zeolite: batch and column studies. *Alex Eng J.* 2022;61(6):4189-207. <http://dx.doi.org/10.1016/j.aej.2021.09.041>.
- Vasiraja N, Prabhakar RSS, Joshua A. Preparation and physio: chemical characterisation of activated carbon derived from prosopis juliflora stem for the removal of methylene blue dye and heavy metal containing textile industry effluent. *J Clean Prod.* 2023;397:136579. <http://dx.doi.org/10.1016/j.jclepro.2023.136579>.
- Tanabe K. Catalytic application of niobium compounds. *Catal Today.* 2003;78(1-4):65-77. [http://dx.doi.org/10.1016/S0920-5861\(02\)00343-7](http://dx.doi.org/10.1016/S0920-5861(02)00343-7).
- Guerrero-Pérez MO. The fascinating effect of niobium as catalytic promoting agent. *Catal Today.* 2020;354:19-25. <http://dx.doi.org/10.1016/j.cattod.2019.04.008>.



11. Rojas E, Delgado JJ, Guerrero-Pérez MO, Bañares MA. Performance of NiO and Ni–Nb–O active phases during the ethane ammoxidation into acetonitrile. *Catal Sci Technol*. 2013;3(12):3173. <http://dx.doi.org/10.1039/c3cy00415e>.
12. Jasim AM, Xu G, Al-Salihi S, Xing Y. Dense niobium oxide coating on carbon black as a support to platinum electrocatalyst for oxygen reduction. *ChemistrySelect*. 2020;5(37):11431-7. <http://dx.doi.org/10.1002/slct.202003225>.
13. Li Y, Yan S, Qian L, Yang W, Xie Z, Chen Q, et al. Effect of tin on Nb<sub>2</sub>O<sub>5</sub>/α-Al<sub>2</sub>O<sub>3</sub> catalyst for ethylene oxide hydration. *J Catal*. 2006;241(1):173-9. <http://dx.doi.org/10.1016/j.jcat.2006.04.030>.
14. Lopes OF, Paris EC, Ribeiro C. Synthesis of Nb<sub>2</sub>O<sub>5</sub> nanoparticles through the oxidant peroxide method applied to organic pollutant photodegradation: a mechanistic study. *Appl Catal B*. 2014;144:800-8. <http://dx.doi.org/10.1016/j.apcatb.2013.08.031>.
15. Costa LM, Ribeiro ES, Segatelli MG, do Nascimento DR, de Oliveira FM, Tarley CRT. Adsorption studies of Cd(II) onto Al<sub>2</sub>O<sub>3</sub>/Nb<sub>2</sub>O<sub>5</sub> mixed oxide dispersed on silica matrix and its on-line preconcentration and determination by flame atomic absorption spectrometry. *Spectrochim Acta B At Spectrosc*. 2011;66(5):329-37. <http://dx.doi.org/10.1016/j.sab.2011.02.005>.
16. Diniz KM, Gorla FA, Ribeiro ES, Nascimento MBO, Corrêa RJ, Tarley CRT, et al. Preparation of SiO<sub>2</sub>/Nb<sub>2</sub>O<sub>5</sub>/ZnO mixed oxide by sol-gel method and its application for adsorption studies and on-line preconcentration of cobalt ions from aqueous medium. *Chem Eng J*. 2014;239:233-41. <http://dx.doi.org/10.1016/j.cej.2013.11.027>.
17. Yang P, Li J, Bao L, Zhou X, Zhang X, Fan S, et al. Adsorption/catalytic combustion of toxic 1,2-dichloroethane on multifunctional Nb<sub>2</sub>O<sub>5</sub>-TiO<sub>2</sub> composite metal oxides. *Chem Eng J*. 2019;361:1400-10. <http://dx.doi.org/10.1016/j.cej.2018.10.071>.
18. Matsuzawa S, Maneerat C, Hayata Y, Hirakawa T, Negishi N, Sano T. Immobilization of TiO<sub>2</sub> nanoparticles on polymeric substrates by using electrostatic interaction in the aqueous phase. *Appl Catal B*. 2008;83(1-2):39-45. <http://dx.doi.org/10.1016/j.apcatb.2008.01.036>.
19. Dutra RPS, de Araújo Pontes LR. Obtenção e análise de cerâmicas porosas com a incorporação de produtos orgânicos ao corpo cerâmico. *Cerâmica*. 2002;48(308):223-30. <http://dx.doi.org/10.1590/S0366-69132002000400010>.
20. Faria FP, Ruellas TMO, del Roveri C, et al. Obtaining porous zinc oxide ceramics using replica technique: application in photocatalysis. *Mater Res*. 2022;25: e20210083. <http://dx.doi.org/10.1590/1980-5373-mr-2021-0083>.
21. Zuoa F, Saunier S, Marinel S, Chanin-Lambert P, Peillon N, Goeuriot D. Investigation of the mechanism(s) controlling microwave sintering of α-alumina: influence of the powder parameters on the grain growth, thermodynamics and densification kinetics. *J Eur Ceram Soc*. 2015;35(3):959-70. <http://dx.doi.org/10.1016/j.jeurceramsoc.2014.10.025>.
22. Holtzberg F, Reisman A, Berry M, Berkenblit M. Chemistry of the group VB pentoxides. VI. The polymorphism of Nb<sub>2</sub>O<sub>5</sub>. *J Am Chem Soc*. 1957;79(9):2039-43. <http://dx.doi.org/10.1021/ja01566a004>.
23. Meert R, Hastenpflug D, Andrade JJO. Contribution to the use of wet sludge water treatment plant fine aggregate in portland cement concretes: evaluation of consistency, density, porosity, absorption, strength and tensile strength. *Materia*. 2021;26(3):e13025.
24. Miyah Y, Lahrichi A, Idrissi M, Boujraf S, Taouda H, Zerrouq F. Assessment of adsorption kinetics for removal potential of Crystal Violet dye from aqueous solutions using Moroccan pyrophyllite. *J Assoc Arab Univ Basic Appl Sci*. 2017;23(1):20-8. <http://dx.doi.org/10.1016/j.jaubas.2016.06.001>.
25. Siqueira Oliveira AM, Paris EC, Giraldo TR. GIS zeolite obtained by the microwave-hydrothermal method: synthesis and evaluation of its adsorptive capacity. *Mater Chem Phys*. 2021;260:124142. <http://dx.doi.org/10.1016/j.matchemphys.2020.124142>.